Report by Working Group WGE - Dynamic Response

Yukio Tamura [a], Ahsan Kareem [b], Giovanni Solari [c], Kenny C. S. Kwok [d], John D. Holmes [e]

[a] *Tokyo Polytechnic University, Atsugi, Kanagawa, Japan*
[b] *University of Notre Dame, Notre Dame, Indiana, USA*
[c] *University of Genova, Via Montallegro, Genoa, Italy*
[d] *Hong Kong University of Science & Technology, Clear Water Bay, Hong Kong*
[e] *JDH Consulting, Mentone, Victoria, Australia*

ABSTRACT: This paper describes the progress report of the IAWE Working Group WGE - Dynamic Response, one of the International Codification Working Groups set up at ICWE10 in Copenhagen.

KEYWORDS: gust loading factor, wind load combination, wind spectra, building dynamic characteristics

1 INTRODUCTION

Working Group E was set up at the First International Codification Workshop held in Bochum, Germany on September 15th 2000 to concentrate discussion on problems related to dynamic response. The aim of the Codification Workshop is to encourage and facilitate more commonality in national, regional and international wind load codes and standards. WGE met once at the Second International Codification Workshop immediately following the Fifth Asia-Pacific Conference on Wind Engineering held in Kyoto from October 22 - 24, 2001.

The following are the members of sub-group WGE (Dynamic Response): Y. Tamura (Japan) Convenor, D. Boggs (U.S), A. Kareem (U.S.), H. Katsuchi (Japan), K. Kwok (Hong Kong), W. Melbourne (Australia), K. Handa (Sweden), J.D.Holmes (Australia), and G. Solari (Italy).

WGE met once at the Second International Codification Workshop immediately following the Fifth Asia-Pacific Conference on Wind Engineering held in Kyoto from October 22 - 24, 2001. Approximately 40 persons attended this meeting, and the following eight presentations were made:

- Expected improvements to the new Hong Kong Code (K.C.S. Kwok);
- Revision work for the AIJ Recommendations (Y. Tamura, H. Kawai and T. Ohkuma);
- Codification of acceleration criteria in Australia (W.H. Melbourne);
- 3-D gust effect factor and equivalent static forces (G. Solari);
- A new gust loading factor approach (A. Kareem);
- Comparison of wind spectra for along-wind response calculation (J.D. Holmes);
- Wind-resistant design of road bridges (H.Sato); and
- Monitoring of Honshu-Shikoku bridges (H. Katsuchi).
- Application of CFD to design (T. Tamura);
- Category and topography corrections for directional extreme wind speeds (J. Kanda); and
- Directionality of thunderstorm winds (E. Choi).

Then, discussions were held to confirm common understanding of methods for predicting wind-induced dynamic responses of buildings and structures, with the view to making recommendations to the ISO Working Group (TC98/SC3/WG2) meeting the following day for revision of the International Standard for Wind Actions (ISO4354).

This report was written by Y. Tamura (Sections 1, 4 and 7), A. Kareem (Sections 2 and 3.2), G. Solari (Section 3.1), K.C.S. Kwok (Section 5) and J.D. Holmes (Section 6).

2 COMPARISONS OF GLFS AND WIND-INDUCED RESPONSE OF MAJOR CODES AND STANDARDS

There have been several comparative studies on dynamic responses estimated by codes, e.g. Kijewski & Kareem (1998)[1], Hui et al. (2001)[2], Zhou et al. (2002)[3], and Asami (2002)[4]. Different definitions of the design wind speed, e.g. hourly mean, 10-min mean, and 3s-gust, different terrain categories and different mean wind profiles and turbulence intensity/scale profiles make these comparisons quite difficult. In these studies, conversions were introduced to enable these comparisons, and thus enabled a careful evaluation of the results based on different standards. The differences and the commonalities in the provisions for the dynamic response in the major codes and standards are cataloged in these studies. A short summary is presented here.

A comprehensive comparison of the along-wind loads and their effects on tall buildings was conducted utilizing the major international codes and standards: the US Standard (ASCE 7-98, 2000 [5]), the Australian Standard (AS1170.2, 1989 [6]), the National Building Code of Canada (NBCC, 1995 [7]), the Architectural Institute of Japan Recommendations (AIJ-RLB, 1993 [8]) and the European Standard (Eurocode ENV1991-2-4 [9]). These codes and standards utilize some form of the traditional displacement-based gust loading factor for assessing the dynamic along-wind loads and their effects on tall structures. Although deriving themselves from a similar theoretical basis, considerable scatter in the predictions of codes and standards have been reported, e.g. Kijewski & Kareem [1]. Unfortunately, the globalization of the construction industry and the prospect of developing unified international codes and standards make it increasingly important to better understand the underlying differences, prompting an in-depth investigation by Zhou et al. (2002) [10]. It was found that the varying definitions of wind field characteristics, including mean wind velocity profile, turbulence intensity profile, wind spectrum, turbulence length scale, and wind correlation structure, were the primary contributors to the scatter in predicted response quantities. An example presented in Zhou et al. [10] highlights these differences..

3 3-D GEF AND GLF TECHNIQUES

3.1 *3-D GEF based on mean static force distribution in the along-wind direction*

Original studies on the dynamic alongwind response of structures (Davenport, 1967 [11], Simiu, 1976 [12], Solari, 1982 [13]) expressed the maximum displacement as the product of the mean static displacement by a non-dimensional constant coefficient, the Gust Response Factor (GRF), calculated by taking into account only the first mode of vibration. These also defined the Equivalent Static Force (ESF) as the force that statically applied on the structure produces the maximum displacement. Exploiting structural linearity, this force was assigned as the product of the mean static force by the GRF.

Further researches developed two distinct lines. The first was aimed at evaluating maximum effects due to the along-wind response by using the load response correlation method

(Kasperski, 1992 [14]), the influence function technique (Davenport, 1995 [15]), suitable along-wind Gust Effect Factors (GEF) (Zhou & Kareem, 2001 [16]) and loading combination procedures (Holmes, 2002 [17]). The second generalised the original criteria from the along-wind response to the crosswind and torsional responses, by fitting the results of wind tunnel tests (Tamura et al., 1996 [18] and Zhou et al., 2003 [19]) or by developing analytical methods based on a so-called 3-D GRF (Piccardo & Solari, 2000 [20]).

The 3-D GEF technique (Piccardo & Solari, 2002 [21]) creates a general framework that represents the junction point of these two research lines and involves, as particular cases, most of the previous approaches.

Consider a cantilever vertical structure whose height h is much greater than the reference size b of its cross-section. Let x,y,z be a Cartesian reference system; z coincides with the structural axis and is directed upwards; x,y are coplanar with ground; x is aligned with the mean wind direction. The structure has linear elastic behavior and three un-coupled components of motion, the alongwind and crosswind displacements, towards x,y, and the θ torsional rotation, around z. Let e_α be a generic load effect at level r, associated with the generalized α direction of the motion. Its maximum value and the related ESF are given by the relationships:

$$\overline{e}_{\alpha,\max}(r) = \overline{e}_\alpha^x(r) G_\alpha^e(r) \tag{1}$$

$$F_{\alpha eq}^e(z,r) = \lambda_\alpha G_\alpha^e(r) \overline{F}_x(z) \tag{2}$$

where $\overline{F}_x$ is the mean static force in the alongwind direction; $\overline{e}_\alpha^x$ is the static effect due to the application of the generalized force $\lambda_\alpha \overline{F}_x$ in the α direction, where $\lambda_x = \lambda_y = 1$, $\lambda_\theta = b$; G_α^e is a non-dimensional quantity referred to as the 3-D GEF. It is furnished by:

$$G_\alpha^e(r) = \mu_\alpha^e(r) + g_\alpha^e(r)\sqrt{Q_\alpha^e(r) + D_\alpha^e(r)} \tag{3}$$

where $\mu_\alpha^e, Q_\alpha^e, D_\alpha^e$ are non-dimensional quantities referred to as, respectively, the static, quasi-static and resonant terms of the effect:

$$\mu_\alpha^e(r) = \frac{\overline{e}_\alpha(r)}{\overline{e}_\alpha^x(r)} \quad ; \quad Q_\alpha^e(r) = \frac{\left[\sigma_{Q\alpha}^e(r)\right]^2}{\left[\overline{e}_\alpha^x(r)\right]^2} \; ; \; D_\alpha^e(r) = \frac{\left[\sigma_{D\alpha}^e(r)\right]^2}{\left[\overline{e}_\alpha^x(r)\right]^2} \tag{4}$$

$\overline{e}_\alpha$ is the mean static value of e_α; $\sigma_{Q\alpha}^e, \sigma_{D\alpha}^e$ are the root mean square values of the quasi-static and resonant parts of e_α; g_α^e is the peak factor. The static and quasi-static terms $\overline{e}_\alpha, \overline{e}_\alpha^x, \sigma_{Q\alpha}^e$ are evaluated by the influence function technique. The resonant term $\sigma_{D\alpha}^e$ is determined assuming that the resonant response in the α direction only depends on the related first mode of vibration. Closed form solutions of G_α^e are given in Piccardo & Solari [21]. Solari & Repetto (2002) [22] introduces a method to classify vertical structures into homogeneous categories, and assess structural tendencies due to gust buffeting.

It is worth notice that, when e_α denotes generalised displacements, Equations (1)-(3) identify with the 3-D GRF technique (Piccardo & Solari [20]). Moreover, focusing attention on the alongwind response, they coincide with Davenport's original formulae [11]. In other words, the 3-D GEF technique completes the chain of the steps afforded towards the complete generalisation of the original GRF technique including, in one simple quantity, the 3-D GEF, all the information necessary to determine the 3-D gust-excited load effects on cantilever vertical structures.

It is also worth notice that Equation (2) defines the ESFs through one compact formula that implies a unique load pattern, $\overline{F}_x$. In the along-wind and crosswind directions, it is scaled by the along-wind and crosswind GEFs, G_x^e and G_y^e, respectively; in the torsional direction, it is multiplied by the equivalent eccentricity bG_θ^e, G_θ^e being the torsional GEF. This definition is very useful in the engineering sector. Only three static loading conditions, the alongwind force $\overline{F}_x$, the crosswind force $\overline{F}_x$, and the torsional moment $b\overline{F}_x$, are initially applied. The related effects $\overline{e}_x^x$, $\overline{e}_y^x$ and $\overline{e}_\theta^x$ are then derived by equilibrium relationships. Maximum effects are finally obtained by scaling these patterns by the the appropriate 3-D GEF (Eq. 3).

Repetto & Solari (2003) [23] provides a general framework of the procedures developed in literature to evaluate the ESF, discussing the advantages and some limitations of the 3-D GEF technique.

3.2 *3-D GLF based on aerodynamic loading database*

In this section the concept of 3-D Gust Loading Factor for estimating dynamic load components in three directions based on an aerodynamic loading database along the "gust loading factor" format that has generally been used for the along-wind response is provided (Zhou et al. [19]). It is envisaged that the new formulation will be most appropriate for inclusion in codes and standards and also serves as a convenient format for the interpretation of wind tunnel test results.

The proposed 3-D GLF is an extension of the GLF concept based on the base bending moment or base torque response defined as

$$G = \hat{\boldsymbol{M}} / \overline{M}' \tag{5}$$

where G = GLF; $\overline{M}'$ = reference mean base bending moment or base torque, which can be computed for the sway and torsional modes, respectively, by

$$\overline{M}'_{D,L} = \int_0^H \overline{P}(z) \cdot z \cdot dz \tag{6}$$

$$\overline{M}'_T = \int_0^H \overline{P}(z) \cdot (0.04 \cdot B) dz \tag{7}$$

where $\overline{P}(z)$ = mean along-wind load at any height *z* above the ground; and *H* and *B* = building height and width normal to the oncoming wind, respectively. Subscripts *D, L* and *T* represent the along-wind, crosswind and torsional directions, respectively. If not specifically indicated, the given formulation would be applicable to all three directions. The reference mean base moment in Equation (6) in the crosswind and the base torque in Equation (7) are not the actual mean base moments that act on the building. Usually, for most symmetrical buildings, the mean base moments in the crosswind and torsional directions are either very small or zero. The reference mean torque in Equation (7) corresponds to the overall torsional effect of a partial load with 25% reduction in any portion of the building, as recommended in the current ASCE7-98 [5] and NBCC [7] (Isyumov & Case, 2000 [24]; Boggs et al., 2000 [25]; Xie and Irwin 2000 [26]; Zhou & Kareem, 2000 [27]).

For convenience, the reference mean base moment in the crosswind is set equal to the along-wind mean base moment. $\hat{\boldsymbol{M}}$ = peak base bending moment or base torque response which can be expressed as

$$\hat{\boldsymbol{M}} = \overline{M} + g \cdot \sigma_{\boldsymbol{M}} \tag{8}$$

where $\overline{M}$ = mean base bending moment or base torque; g = peak factor, which is usually around 3 ~ 4; and $\sigma_{\boldsymbol{M}} = \left(\int_0^\infty S_{\boldsymbol{M}}(f) df \right)^{1/2}$ = root mean square (RMS) of the base bending moment and base torque response, and $S_{\boldsymbol{M}}(f)$ = power spectral density (PSD) of the fluctuating base moment or torque response. It has been a general practice to divide the integration term of the fluctuating response into two portions

$$\sigma_{\boldsymbol{M}} = \sqrt{\sigma_{\boldsymbol{M}B}^2 + \sigma_{\boldsymbol{M}R}^2} \tag{9}$$

in which $\sigma_{\boldsymbol{M}B}$ and $\sigma_{\boldsymbol{M}R}$ = background and resonant components of the base bending moment or base torque response, respectively. Thus, the 3-D GLF can be expressed in the form

$$G = \overline{G} + \sqrt{G_B^2 + G_R^2} \tag{10}$$

where $\overline{G}$, G_B and G_R = mean, background and resonant components of the GLF, respectively, which can be computed by

$$\overline{G} = \overline{M} / \overline{M}' \tag{11}$$

$$G_B = g_B \cdot \sigma_{\boldsymbol{M}B} / \overline{M}' \tag{12}$$

$$G_R = g_R \cdot \sigma_{\boldsymbol{M}R} / \overline{M}' \tag{13}$$

where $g_B = g_u$ = background peak factor or peak factor for the fluctuating wind velocity as suggested in ASCE7-98 [5]. It is important to note that when applying to the along-wind response, the preceding 3-D GLF reduces exactly to the same result as given in a new GLF model by Zhou and Kareem [16]. This new GLF model has the advantage of offering an improved GLF format that reflects more accurately the description of dynamic load effects on structures in comparison with the traditional GLF approach as used in current codes and standards. For the along-wind response, the mean component of the GLF is unity; and for the crosswind and torsional response of a symmetrical building, it is usually very small or zero. The calculation for the background and resonant components of the base bending moment response will be provided in the following sections.

3.2.1 *Base moments response and mode shape corrections*

Most GLF based approaches involve the generalized wind loading, which has been observed to be quite sensitive to the mode shape exponent and the aerodynamic pressure field characteristics (e.g., Zhou et al. [10]). These parameters in engineering practice are either unknown or can only be estimated approximately. For a particular engineering application, the mode shape correction of the generalized wind load scheme may introduce significant uncertainty depending on the parameters involved. On the other hand, it is noted that a base-bending-moment-based procedure can notably reduce the analysis efforts. The PSD of the fluctuating base bending moment or base torque response can be evaluated using the following equation:

$$S_{\boldsymbol{M}}(f) = \eta_{\boldsymbol{M}} \cdot S_M(f) \cdot \left|H_1(f)\right|^2 \tag{14}$$

where $\eta_{\boldsymbol{M}}$ = mode shape correction for the base moments and torque response. For the background response, both $\left|H_1(f)\right|^2$ and $\eta_{\boldsymbol{M}}$ are equal to unity. When a building has an ideal mode shape, i.e., linear in sway modes and uniform in torsional direction, $\eta_{\boldsymbol{M}}$ for the resonant response component is also equal to unity (Boggs & Peterka, 1989 [28], Zhou & Kareem [16], Zhou et al. [10]). In addition, studies have shown that, unlike the procedure based on the generalized wind load, the mode shape correction $\eta_{\boldsymbol{M}}$ for the base moments is relatively insensitive to the non-ideal mode shape, mass distribution and aerodynamic pressure field characteristics. For a wide range of involved parameters, the mode shape correction can be neglected in the base-moments based approach, which results in acceptable error in the overall wind-induced response estimates (Zhou & Kareem [16], Zhou et al. [3]). It is noteworthy that the same symbol but expressed in bold is employed in Equation (14) to distinguish the base moment or base torque response from the externally applied aerodynamic moment or torque. The former includes the dynamic magnification effects resulting from wind fluctuations and structural dynamics.

Using Equation (14), the definition of the background response, and the white-noise excitation assumption, the background and resonant components of the base moments can be computed, respectively, by

$$\sigma_{\boldsymbol{M}B} = \sigma_M \tag{15}$$

$$\sigma_{\boldsymbol{M}R} = \sqrt{\frac{\pi f_1}{4\zeta_1} \cdot S_M(f_1)} \tag{16}$$

3.2.2 *Aerodynamic base moment database*

Though a host of HFBB data on wide variety of structures has been collected in laboratories worldwide, it has not been assimilated and made accessible to the global community, to fully realize it's potential. Fortunately, the Internet now provides the opportunity to pool and archive the international stores of wind tunnel data. The first step toward an "e-database" of aerodynamic wind loads was introduced by Zhou et al. [19], based on HFBB measurements on a host of isolated tall building models, and is currently accessible to the worldwide Internet community via Microsoft Explorer at the URL address http://www.nd.edu/~nathaz. Through the use of this interactive portal, users can select the geometry and dimensions of a model building, from the available choices, and specify an urban or suburban condition. Upon doing so, the aerodynamic load spectra for the along-wind, crosswind or torsional response is displayed with a Java interface permitting users to specify a reduced frequency of interest and automatically obtain the corresponding spectral value. When coupled with the supporting web documentation, examples and concise analysis procedure based on the base bending moment, the database provides a comprehensive tool for computation of the wind-induced response of tall buildings, suitable for possible inclusion in codes and standards as a design guide in the preliminary stages.

The aerodynamic base moments involve complex fluid-structure interactions, which can only be determined accurately with wind tunnel tests except for the along-wind direction, where the strip and quasi-steady theories are usually assumed. For the crosswind and torsional directions, there has not been, to date, any acceptable analytical procedure to determine this information based on the oncoming velocity fluctuations and building geometry. The base moment in a non-dimensional form can be obtained from the HFBB (Tschanz & Davenport, 1983 [29], Boggs & Peterka [28]) or simultaneously monitored surface pressure measurements on scaled building models (e.g., Kareem 1982 [30], Ho, et al., 1999 [31]).

In this database, the measured aerodynamic base moments are reduced in the following non-dimensional formats:

$$\sigma_{C_M} = \sigma_M / M' \tag{17}$$

$$C_M(f) = \left(f \cdot S_M(f)\right) / \sigma_M^2 \tag{18}$$

where M' = reference moment or torque in the test, which is defined by $M'_D = \left(1/2\rho \overline{U}_H^2 BH^2\right)$, $M'_L = \left(1/2\rho \overline{U}_H^2 DH^2\right)$ and $M'_T = \left(1/2\rho \overline{U}_H^2 BDH\right)$ for the along-wind, crosswind and torsional directions, respectively. The non-dimensional data can be directly used in the response analysis of buildings. It is important to note the manner in which the reference moments have been defined in this database, e.g., the crosswind moment is non-dimensionalized with respect to D, which is the crosswind face dimension.

3.2.3 *Evaluation of the 3-D GLF*

Given the aerodynamic base moments, the three components of 3-D GLF can be evaluated by substituting Equations (15) - (18) into Equations (11) – (13) as

$$\overline{G} = \begin{cases} 1 & \text{for along-wind;} \\ 0 & \text{for crosswind and torsion for symmetric buildings} \end{cases} \tag{19}$$

$$G_B = g_B \cdot \sigma_{CM} \cdot M' / \overline{M'} \tag{20}$$

$$G_R = g_R \frac{\sigma_{CM} \cdot M'}{\overline{M'}} \sqrt{\frac{\pi \cdot C_M(f_1)}{4\zeta_1}} \tag{21}$$

3.2.4 *Application of 3-D GLF in design*

Among other advantages, the base moment response based GLF, as outlined here exhibits a notable feature that the ESWL on a building can be obtained by distributing the base moment response to each floor. For the mean and background components, the ESWLs can be expressed by

$$\overline{\boldsymbol{P}}_i = \overline{\boldsymbol{M}} \cdot \frac{2+2\alpha}{H^2} \cdot \left(\frac{z_i}{H}\right)^{2\alpha} \cdot \Delta H_i \tag{22}$$

$$\hat{\boldsymbol{P}}_{Bi\,D,L} = \hat{\boldsymbol{M}}_{B\,D,L} \cdot \frac{2+2\alpha}{H^2} \cdot \left(\frac{z_i}{H}\right)^{2\alpha} \cdot \Delta H_i \tag{23}$$

$$\hat{\boldsymbol{P}}_{BiT} = \hat{\boldsymbol{M}}_{BT} \cdot \frac{1+2\alpha}{H} \cdot \left(\frac{z_i}{H}\right)^{2\alpha} \cdot \Delta H_i \tag{24}$$

For the resonant components, the ESWL in sway modes is given by

$$\hat{\boldsymbol{P}}_{Ri\,D,L} = \hat{\boldsymbol{M}}_{R\,D,L} \cdot \frac{m_i \varphi_{1i\,D,L}}{\sum m_i z_i \varphi_{1i\,D,L}} \tag{25}$$

and the torsional mode

$$\hat{\boldsymbol{P}}_{RiT} = \hat{\boldsymbol{M}}_{RT} \cdot \frac{I_i \varphi_{1iT}}{\sum I_i \varphi_{1iT}} \tag{26}$$

where $\overline{\boldsymbol{P}}$ = ESWL; $\overline{\boldsymbol{M}} = \overline{G} \cdot \overline{M'}$, $\hat{\boldsymbol{M}}_B = G_B \cdot \overline{M'}$ and $\hat{\boldsymbol{M}}_R = G_R \cdot \overline{M'}$ = mean, background and resonant base moment components, respectively; z_i = elevation of the ith floor above the ground; $\Delta H_i = z_i - z_{i-1}$ = floor height of the ith floor; and m_i, I_i and φ_{1i} = mass, mass moment of inertia and first mode shape at the ith floor height, respectively.

Any wind load effects such as the internal forces in each member, as well as the overall deflection and acceleration, can be computed expediently through a simple analysis utilizing these ESWLs. For example, the acceleration response estimated for serviceability checking procedure can be evaluated using only the resonant ESWL component.

4 COMBINATIONS OF WIND LOAD EFFECTS

Wind load combinations must be considered in design, especially when wind directionality is taken into account. Melbourne (1975) [32], Vickery & Basu (1984) [33], Solari & Pagnini (1999) [34], Tamura et al., (2002) [35][36] and Kikuchi et al. (2003) [37] examined the dynamic characteristics of wind force components and response components and discussed the combinations of wind load effects.

AS1170.2 [6] gives a formula for peak resultant vector moment, where it is assumed that the peak resultant base moment is equal to the peak along-wind moment when the mean crosswind response is equal to zero and the crosswind dynamic response is less than or equal to the along-wind response. A new standard AS/NZS 1170.2 (2002) [38] gives a formula for estimating the total scalar effect ε_t such as an axial load in a column as:

$$\varepsilon_t = \varepsilon_{am} + \sqrt{\varepsilon_{ap}^2 + \varepsilon_{cp}^2} \tag{27}$$

where ε_{am} is the load effect due to the mean along-wind action, ε_{ap} is that due to the peak along-wind action, and ε_{cp} is that due to the peak crosswind action, where it estimates double the mean along-wind effect. ASCE7-98 [5] gives simple wind load combinations for buildings higher than 60ft, where 75% of along-wind load and the same values are simultaneously applied in the crosswind direction, and the torsional load is also taken into account as in its previous version.

The draft AIJ Recommendations gives two methods. The first is applicable even for the case without information on crosswind or torsional responses. It proposes a wind load combination factor γ defined as:

$$F_L = \gamma F_D \tag{28}$$

which is the crosswind force applied with the design along-wind load. This method is based on the results by Tamura et al. [35][36] and Kikuchi et al. [37]. The combination factor is given as

$$\gamma = 0.34\frac{D}{B} + 0.05 \tag{29}$$

where D and B are the along-wind and crosswind dimensions of a building plan. Another method gives the load combination factor defined as a function of the correlation coefficient between the crosswind response and the torsional response based on Asami (2000) [39].

5 DYNAMIC STRUCTURAL CHARACTERISTICS

Many modern wind load standards contain procedures for the calculation of dynamic wind load and wind-induced response of wind-sensitive structures, including flexible and lightly damped tall buildings. Typically, wind-sensitive structures are those with a first-mode natural frequency less than 1 Hz and a slenderness (height to breadth or depth) ratio greater than four to five.

The natural frequencies of vibration and structural damping ratios, particularly of the fundamental mode of vibration, are the most important structural parameters in the calculation of the dynamic wind load and wind-induced response of wind-sensitive structures. The natural frequency is used in conjunction with the building dimension and the design wind speed to define the design reduced wind velocity, which in turn specifies the wind excitation energy available to cause resonant type response in the building. Through the mechanical admittance function, the degree of dynamic amplification of this available energy into resonant type response depends on the structural damping ratio. Most standards that contain a dynamic calculation procedure provide relatively simple guidelines on the estimation of natural frequencies of vibration and suggested values of structural damping ratio to facilitate the design process.

Most standards provide relatively simple equations for the estimation of natural frequencies of vibration based on the building height or number of stories. The Australian and New Zealand Standard AS/NZS 1170.2 [38], Eurocode ENV1991-2-4 [9], Hong Kong Code of Practice on Wind Effects Draft (1996) [40], and others adopted Equation (30) for all building types:

$$n_1 = \frac{46}{H} \tag{30}$$

in which n_1 is the natural frequency of the fundamental mode of vibration and H is the building height in m. The UK Standard BS6399 (1997) [41] uses a similar equation with a coefficient of 60 and a representative height. The American standard ACSE7-98 [5] also uses a similar equation but adopts different coefficients based on building type. The Chinese Standard GB50009 (2001) [42] uses a simple equation based on number of stories and also adopts coefficients based on building types. GB50009 also suggests a more refined procedure based on building height and width when the structural form is known.

A comprehensive review of the damping in buildings has been reported by Tamura et al (2000) [43]. A selection of design damping ratios currently used in some countries for the full range of buildings including steel and reinforced concrete buildings is presented in Figure 1. Values suggested in some recently revised standards, including AS/NZS 1170.2 [38] and GB50009 [42], and proposed revisions such as the Draft AIJ Recommendations are included in Figure 1 for comparison.

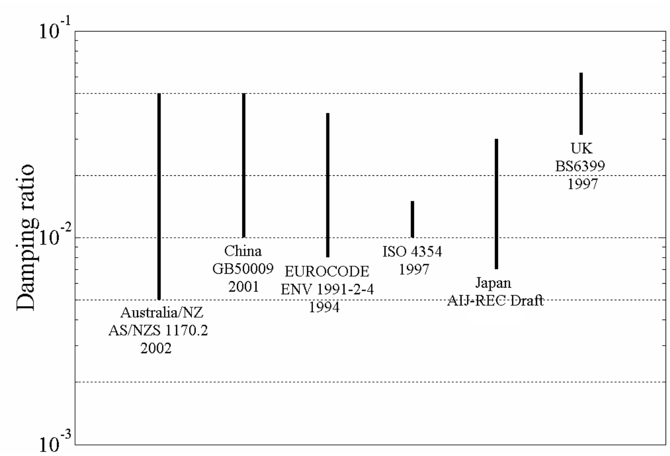

Deleted: ¶

Figure 1. Design damping ratios for tall buildings

Generally, steel buildings have a lower natural frequency and a lower damping ratio than reinforced concrete buildings of a similar height. However, as is expected, the method of estimating natural frequency and in particular the suggested damping ratios vary quite significantly amongst the different standards. As a result, the calculated wind load and wind-induced response, even for identical buildings, will vary correspondingly, according to the standard used for the calculation.

6 WIND SPECTRA FOR ALONG-WIND RESPONSE CALCULATION

6.1 *Mathematical forms*

The following mathematical forms for along-wind velocity spectra are currently used in major current, or recent, wind code and standards :

$$\frac{nS_u(n)}{\sigma_u^2} = \frac{4\left(\frac{n\ell_u}{\overline{U}}\right)}{\left[1+70.8\left(\frac{n\ell_u}{\overline{U}}\right)^2\right]^{\frac{5}{6}}} \quad \text{(von Karman)} \tag{31}$$

$$\frac{nS_u(n)}{\sigma_u^2} = \frac{a_1\left(\frac{n\ell_u}{\overline{U}}\right)}{\left[1+a_2\left(\frac{n\ell_u}{\overline{U}}\right)\right]^{\frac{5}{3}}} \quad \text{(Kaimal)} \tag{32}$$

$$\frac{nS_u(n)}{\sigma_u^2} = \frac{0.67\left(\frac{nL}{\overline{U}}\right)^2}{\left[1+\left(\frac{nL}{\overline{U}}\right)^2\right]^{\frac{4}{3}}} \quad \text{(Davenport)} \tag{33}$$

$$\frac{nS_u(n)}{\sigma_u^2} = \frac{0.6\left(\frac{nL}{\overline{U}}\right)^2}{\left[2+\left(\frac{nL}{\overline{U}}\right)^2\right]^{\frac{5}{6}}} \quad \text{(Harris)} \tag{34}$$

These forms differ primarily in the exponent used in the denominator. The length scale, ℓ_u , is the integral length scale. L is a different length scale used specifically in the Davenport and Harris spectra. The Harris form can be shown to be nearly identical to the von Karman form if L is taken as 11.9 ℓ_u . Table 1 summarizes which standards and codes have used the various forms of along-wind spectra.

Table 1 Spectral densities used in various major wind codes or standards

Code/Standard	Form of along-wind spectral density used
AIJ-RLB [8], Japan	von Karman
AS1170.2 [6], Australia	Harris
AS/NZS1170.2 [38], Australia / New Zealand	Von Karman
ASCE7-98 [5], United States	modified Kaimal
Draft Eurocode ENV1991-2-4 [9], Europe	modified Kaimal
NBCC [7], Canada	Davenport

6.2 *Properties of spectra*

The following properties of any empirical mathematical form of spectral density are desirable, if not essential :

i) $$\int_0^\infty \frac{S_u(n)}{\sigma_u^2}\,dn = 1 \tag{35}$$

- this requirement ensures that the area under the $S_u(n)$ versus n graph equals the total variance of fluctuating wind speed, and is then consistent with the turbulence intensity

ii) $$S_u(0) = 4\sigma_u^2 \frac{\ell_u}{\overline{U}} \tag{36}$$

- this can be derived from the Wiener-Khintchine relations between autocorrelation and spectral density, where the integral scale, ℓ_u, is defined by the area under the auto correlation function :

$$\ell_u = \overline{U}.\int_0^\infty R(\tau)\,d\tau \tag{37}$$

iii) $$\frac{nS_u(n)}{\sigma_u^2} = A\left(\frac{n\ell_u}{\overline{U}}\right)^{-\frac{2}{3}} \quad \text{at high frequencies, where } A \text{ is in the range 0.10 to 0.15} \tag{38}$$

- this is derived from dimensional analysis for the inertial sub-range, and measurements of atmospheric turbulence to determine the factor, A. This frequency range includes the natural frequency range of most tall buildings.

Traditionally, property (ii) has been regarded as less important than the other two. The von Karman form (Eq. (31)) satisfies all three properties, (i), (ii) and (iii). In the case of (iii), the constant A is equal to 0.12.

The Kaimal form, as given in Equation (32), satisfies property (i) only if the ratio a_1/a_2 is equal to 2/3 (0.67). Property (ii) is also satisfied if a_1 is equal to 4, and a_2 is equal to 6. However for those values, the constant A in Equation (38) is equal to 0.20, i.e. a value outside the desirable range. In the draft Eurocode ENV1991-2-4 [9], the values of a_1 and a_2 selected are 6.8 and 10.2, respectively – then (i) is satisfied but (ii) is not; (iii) is satisfied with a value of A of 0.14.

In the case of the Davenport spectrum, (i) is satisfied. (ii) is not satisfied since $S_u(0)$ is equal to 0. Assuming, that the length scale, L, used in this spectrum is equal to 11.9 ℓ_u, then property (iii) is satisfied with A equal to 0.13.

Recommendation. Although all three spectral forms in current use satisfy the more important properties (i) and (iii), only the von Karman form satisfies all three properties, and is the preferred form by WGE. This form is currently used in the AIJ-RLB [8], and in the current AS/NZS1170.2 [38].

7 RECOMMENDATIONS AGREED AT WGE MEETING IN KYOTO

- Gust loading factor calculations in codes should focus on base bending moment rather than on deflections, and
- The von Karman form is generally preferable as the spectrum for along-wind response calculations.

8 REFERENCES

1. T. Kijewski and A. Kareem, Dynamic wind effects: a comparative study of provisions in codes and standards with wind tunnel data, Wind and Structures, An International Journal, Vol.1 (1), 1998, pp.77-109
2. Z. Hui, A. Bachmann and C.A. Graubner, Wind loads on high-rise structures - Comparative study of code provisions according to EUROCODE1 and Chinese Code, Proc. APCWE V, Kyoto, Japan, 2001, pp.613-616
3. Y. Zhou, T. Kijewski and A. Kareem, Along-wind load effects on tall buildings: a comparative study of major international codes and standards, Journal of Structural Engineering, ASCE, 128 (6), 2002, pp.788-796.
4. Y. Asami, Comarisons of gust loading factors in codes and standards, Japanese Domestic Committee on TC98/SC3/WG2 for ISO4354 Revision, 2002, pp.5
5. ASCE7-98, Minimum design loads for buildings and other structures, American Society of Civil Engineers, Reston, VA, 2000
6. AS1170.2, SAA Loading Code, Part 2- Wind forces, AS1170.2-89, Australian Standards, 1989
7. NBCC, User's Guide-NBC1995 Structural Commentaries (Part 4), 1995
8. AIJ-RLB, Recommendations for Loads on Buildings, Architectural Institute of Japan, 1993 (English version, 1996)
9. Eurocode ENV1991-2-4, EUROCODE 1: Basis of Design and Actions on Structures, Part 2.4: Wind Actions, CEN/TC 250/Sc1, 1994
10. Y. Zhou, A. Kareem and M. Gu, On the mode shape corrections for wind load effects on tall buildings, Journal of Engineering Mechanics, ASCE, Vol.128 (1), 2002, pp.15-23.
11. A.G. Davenport, Gust loading factors, Journal of Structural Division, ASCE, Vol.93, 1967, pp.11-34.
12. E. Simiu, Equivalent static wind loads for tall buildings design, Journal of the Structural Division, ASCE, Vol.102, 1976, pp.719-737.
13. G. Solari, Alongwind response estimation: closed form solution, Journal of the Structural Division, ASCE, Vol.108, 1982, pp.225-244.
14. M. Kasperski, Extreme wind load distributions for linear and nonlinear design, Engineering Structures, Vol.14, 1992, pp.27-34.
15. A.G. Davenport, How can we simplify and generalize wind loads, Journal of Wind Engineering and Industrial Aerodynamics, Vols.54-55, 1995, pp.657-669.
16. Y. Zhou and A. Kareem, Gust loading factor: new model, Journal of Structural Engineering, ASCE, Vol.127(2), 2001, pp.168-175.
17. J.D. Holmes, Effective static load distributions in wind engineering, Journal of Wind Engineering and Industrial Aerodynamics, Vol.90, 2002, pp.91-109.
18. Y. Tamura, H. Kawai, Y. Uematsu, H. Marukawa, K. Fujii, Y. Taniike, Wind loads and wind-induced response estimations in the Recommendations for loads on buildings, AIJ 1993, Engineering Structures, Vol.18, 1996, pp.399-411.
19. Y. Zhou, T. Kijewski and A. Kareem, Aerodynamic loads on tall buildings: an interactive database, Journal of Structural Engineering, ASCE, Vol.129 (3), 2003, pp.394-404.
20. G. Piccardo and G. Solari, 3-D wind-excited response of slender structures: Closed form solution, Journal of Structural Engineering, ASCE, Vol.126, 2000, pp.936-943.
21. G. Piccardo and G. Solari, 3-D gust effect factor for slender vertical structures, Probabilistic Engineering Mechanics, Vol.17, 2002, pp.143-155.
22. G. Solari and M.P. Repetto, General tendencies and classification of vertical structures under wind loads, Journal of Wind Engineering and Industrial Aerodynamics, Vol.90, 2002, pp.1299-1319.

23. M.P. Repetto and G. Solari, Equivalent static wind actions on vertical structures, Journal of Wind Engineering and Industrial Aerodynamics, 2003, (in press)
24. N. Isyumov and P.C. Case, Wind-induced torsional loads and response of buildings, Proceedings of Structures Congress 2000, Philadelphia, PA, CD-Rom, Ed. Mohamed Elgaaly, ASCE, Reston, Va, 2000.
25. D.W. Boggs, N. Hosoya and L. Cochran, Sources of torsional wind loading on tall buildings, Proceedings of Structures Congress 2000, Philadelphia, PA, CD-Rom, Ed. Mohamed Elgaaly, ASCE, Reston, Va., 2000
26. J. Xie and P.A. Irwin, Key factors for torsional wind response of tall buildings, Proceedings of Structures Congress 2000, Philadelphia, PA, CD-Rom, Ed. Mohamed Elgaaly, ASCE, Reston, Va., 2000
27. Y. Zhou and A. Kareem, Torsional load effects on buildings under wind, Proceedings of Structures Congress 2000, Philadelphia, PA, CD-Rom, Ed. Mohamed Elgaaly, ASCE, Reston, Va., 2000
28. D.W. Boggs and J.A. Peterka, Aerodynamic model tests of tall buildings, Journal of Engineering Mechanics, ASCE, Vol.115(3), 1989, pp.618-635.
29. T. Tschanz and A.G. Davenport, The base balance technique for the determination of dynamic wind loads, Journal of Wind Engineering and Industrial Aerodynamics, Vol.13, 1983, pp.429-439.
30. A. Kareem, Measurements of total dynamic loads from surface pressures, Proceedings of the International Workshop on Wind Tunnel Modeling Criteria and Techniques. Ed. T. A. Reinhold; National Bureau of Standards, Gaithersburg, Maryland, Cambridge University Press, 1982
31. T.C.E. Ho, G.R.Lythe and N. Isyumov, Structural Loads and responses from the integration of instantaneous pressure, Wind Engineering into the 21st Century, Vol. 3 (editors: Larsen, Larose and Livesey), 1999
32. W,H. Melbourne, Probability distributions of response of BHP house to wind action and model comparisons. Journal of Industrial Aerodynamics, Vol.1(2), 1975, pp.167-175.
33. B.J. Vickery and R.I. Basu, The response of reinforced concrete chimneys to vortex shedding. Engineering Structures, Vol.6, 1984, pp.324-333.
34. G. Solari and L.C. Pagnini, Gust buffeting and aeroelastic behaviour of poles and monotubular towers. Journal of Fluid and Structures, Vol.13, 1999, pp.877-905.
35. Y. Tamura, H. Kikuchi and K. Hibi, Quasi-static wind load combinations for low- and middle-rise buildings AGD2002 Symposium Preprints, Engineering Symposium to Honor Alan G. Davenport for His 40 Years of Contributions, The University of Western Ontario, Canada, 2002, pp.C3-1 - C3-12
36. Y. Tamura, H. Kikuchi and K. Hibi, Quasi-static wind load combinations for buildings, The Second International Symposium on Wind and Structures, Busan, Korea, August 21-23, 2002, pp.61-68
37. H. Kikuchi, Y. Tamura and K. Hibi, Quasi-static wind load combinations for low-, middle- and high-rise buildings, Proceedings of the 11th International Conference on Wind Engineering, IAWE, Lubbock, USA, 2003 (in press)
38. AS/NZ1170.2, Australian/New Zealand Standard, Structural design actions, Part 2: wind actions, Standards Australia & Standards New Zealand, 2002
39. Y. Asami, Combination method for wind loads on high-rise buildings, Proceedings of the 16th National Symposium on Wind Engineering, Tokyo, Japan, 2000, pp.531-534
40. Code of practice on wind effects, Hong Kong, Buildings Department, Draft, 1996
41. BS 6399: Part 2, Loading for building Structures. Part 2. Code of practice for wind loads, British Standards Institution, 1997
42. GB50009, Chinese Standard for wind loads, 2001
43. Y. Tamura, K. Suda and A. Sasaki, Damping in buildings for wind resistant design, International Symposium on Wind and Structures for the 21st century, Cheju, Korea, 2000, pp.115-130